On the Origin of Ferromagnetism and the Hyperfine Fields in Fe, Co, and Ni†

Mary Beth Stearns
Scientific Research Staff, Ford Motor Company, Dearborn, Michigan 48121
(Received 29 January 1973)

A specific model for the origin of ferromagnetism in Fe, Co, and Ni is given, which attributes the origin of the ferromagnetism to the indirect coupling of the predominately localized d-like electrons through a small number of itinerant d-like electrons. The model suggests that about 5% of the $3d$ electrons are in itinerant bands and 95% are in d bands which are sufficiently narrow that they can be considered localized. Band-structure calculations and Fermi-surface measurements for Fe strongly support this model. Many other features of the $3d$ transition series are discussed and seen to be consistent with this model. Using this model we give the scaling rules for the three contributions to the hyperfine fields: H_{cp}, the core polarization; H_{ce}, the $4s$-like conduction-electron polarization; and H_v, the volume overlap polarization. We also update the treatment of the volume overlap term and show that the change in sign of the hyperfine field at Sn in Ni as compared with that in Fe and Co results from the competition of the comparable-sized H_{ce} and H_v terms for Sn.

I. INTRODUCTION

The origin of ferromagnetism in Fe has been a fascinating subject of study[1] for many decades. It was originally thought to be due to direct interactions between the Fe atoms, but careful calculations[2] carried out in the early sixties and since have shown that this mechanism is too weak to account for the observed Curie temperature. Another theoretical proposal which gave quantitative predictions was that the ferromagnetism is caused by the indirect Coulomb exchange interaction of the coupling of the spins of the magnetic ions via the conduction electrons. Zener[3] originally considered only the static contribution of the conduction electrons on the magnetization while a number of other authors[4] made more complete second-order perturbation calculations which included the off-diagonal matrix elements. These gave the familiar oscillatory behavior of the spin polarization as a function of distance from a magnetic ion. The usual Ruderman-Kittel-Kasuya-Yosida (RKKY) theories calculate the polarization of the conduction electrons due to s-d exchange. Another type of mechanism which has also been considered is an interaction through s-d interband mixing.[5] The s-like conduction-electron polarization (CEP) can be measured through its hyperfine interaction. This has been done extensively[6,7] and we find in Ref. 7 that both the Coulomb exchange and interband mixing may give comparable contributions to the polarization in the region of the nearest neighbor and that whereas the net polarization of the $4s$ electrons is around -0.005 ± 0.01, they are negatively polarized at the first-(N_1) and second- (N_2) nearest-neighbor distances. Thus, if this interaction were responsible for the magnetic alignment, this negative polarization would dominate and would align Fe antiferromagnetically. Thus we inferred[6(b)] that the ferromagnetism was caused by the indirect coupling of the magnetic ions through some itinerant d electrons. We have recently presented such a model[8] in more detail and have concluded that the Fe d electrons appear to be about 95% or more spacially localized and 5% or less itinerant in character. In Sec. II we present this model in greater detail and show that band calculations[9,10] and Fermi-surface measurements[11] support this picture. The model is similar in one respect to that proposed by Friedel *et al.*,[12] but very different in most assumptions and conclusions as discussed in Sec. II B.

In Sec. III we describe the model for the origin of the hyperfine field in Fe, Co, and Ni and its dilute alloys and give the scaling rules for each of the contributions. In Sec. IV we up-date the evaluation of the H_v term and discuss some particular cases of the systematics of the hyperfine fields. In Sec. V we discuss the hyperfine field at Sn in Fe, Co, and Ni.

II. MODEL FOR THE ORIGIN OF FERROMAGNETISM IN Fe, Co, AND Ni

There is much experimental evidence that the major portion of the Fe moment is spacially localized. This evidence comes from: (i) specific-heat measurements[13] which gave an entropy associated with the transition through the Curie temperature of $Nk\ln 3$; (ii) neutron diffuse-inelastic-scattering experiments[14]; (iii) magnetic-form-factor measurements[15] where the magnetic electrons are seen to have spacial distributions very similar to those calculated for free atoms; (iv) near equality of the high-temperature moment and the saturation moment[16] of Fe; and (v) the comparison of the average moment and the average hyperfine field[8] at Fe nu-

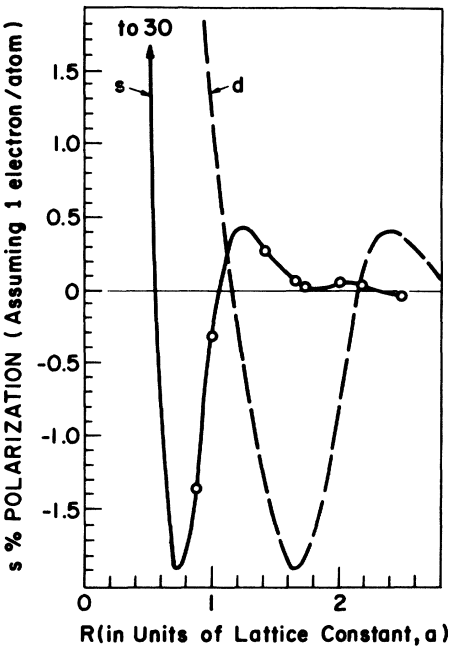

FIG. 1. Measured polarization of the 4s-like electrons in Fe (solid curve). The dashed curve indicates that for the itinerant d-like electrons the first node of the polarization curve must be beyond the N_2 distance. This requires that $k_F^d \leq 0.4$ (in units of $2\pi/a$).

clei upon alloying with small amounts of Si or Al. Calculations have shown that direct interactions between the localized moments are too weak[2] to account for the observed Curie temperature so the ferromagnetism is assumed to arise from indirect coupling of the local moments through the itinerant electrons in Fe.

The polarization of the 4s electrons has been measured directly by observing the hyperfine-field behavior upon alloying.[6,7] The measured polarization is shown in Fig. 1 by the solid curve and data points. Although the net polarization is found to be around $-0.5 \pm 1\%$,[17] the polarization at N_1 and N_2 neighbors is dominant and negative (opposite to the Fe moment) and thus would tend to align Fe antiferromagnetically. Therefore the mechanism responsible for ferromagnetism was inferred to be[6] the indirect exchange interaction of the localized 3d electrons through *a small fraction* of itinerant 3d-like electrons. Although the RKKY-type calculations have been made only for s electrons we will assume here that a similar behavior is applicable for itinerant d-like electrons at N_1 distances and beyond. Indeed, in the asymptotic region we know that the polarization will oscillate in space as $\sim 1/k_F$; however, this is not so obvious in the near-neighbor region but has generally been assumed to be so. For distances of about one-half N_1 and beyond it was found that the CEP curves were not very sensitive to the wave functions used to describe the s electrons[18,19] so we may be justified in treating itinerant d electrons like s electrons far enough out from the origin. Another complication that arises is that the itinerant d electrons may be quite polarized, and so again the RKKY calculations should be extended to polarized electrons. However, for simplicity, ignoring all these difficulties and assuming that the d electrons behave in a manner similar to the s electrons for distances of N_1 and beyond, an upper limit for the fraction of itinerant d's can be estimated from the argument that if these give rise to the ferromagnetism then the first node in the oscillatory polarization curve must be beyond the N_2 distance in Fe (since N_1 and N_2 are so close). This is indicated by the dashed curve in Fig. 1 and since the first node is at $2\,k_F R \simeq 4.8$ for Fe this requires that $k_F \leq 0.4$, in units of $2\pi/a$, where a is the lattice constant. (The k_F value for the 4s electrons was measured to be 0.6.) Another independent estimate of the localized character was made in Ref. 8 by a comparison of the saturation magnetization behavior with the average hyperfine-field behavior for dilute alloys of Al or Si in Fe. The fraction of itinerant d's was estimated from this procedure to be about 5% or less. In terms of a band picture we interpret this as meaning that about 5% or less of the d electrons are in itinerant d bands and about 95% are in d bands sufficiently narrow that they can be considered localized.

A. Comparison with Band-Structure Calculations and Fermi-Surface Measurements of Fe

We now look at band-structure calculations and Fermi-surface measurements to see if they support such a picture. In Fig. 2 we show the band structure of the majority and minority spins for ferromagnetic iron as calculated by Duff and Das (DD).[10] We expect the bands which are to be identified with localized states to be somewhat flat and those which are to be associated with itinerant-electron states to be paraboliclike. Near the center of the Brillouin zone (Γ) this is indeed seen to be the case. Near Γ the lowest state in Fig. 2 is due to s-like electrons and is quite parabolic around Γ. The higher five states are d states and for each type of spin four of the states are seen to be quite flat near Γ while one has a predominant paraboliclike behavior (the top t_{2g} band near Γ). We can further follow the d levels out from Γ and see that indeed they are quite flat over large regions, e.g., between Γ and P or F all but the two "parabolic" d bands are quite flat. Where they obtain appreciable curvature appears to be identifiable with regions of hybridization between the s and d bands. Note in particular the minority-spin bands in the direction Γ-P, Γ-N, and Γ-F. There

the parabolic-d-like band crosses the Fermi level before s-d hybridization appears to occur. Thus in these directions the electrons at the Fermi level can be interpreted as having predominantly $3d$-like character. In the H direction s-d hybridization occurs near the region where the top t_{2g} band crosses the Fermi level. This has been interpreted as corresponding to the electron lens and hole pockets that allow open orbits in the H direction[11] (see Fig. 3). Table I gives the k_F values where the paraboliclike d bands cross the Fermi level from the calculation of DD.[10] We have also listed the number of d-like electrons in the itinerant d bands for each spin direction assuming a nearly-free-electron-like behavior, so $n = (2\pi/3)(k_F a/2\pi)^3$ for a bcc lattice. There will also be some itinerant d-like electrons associated with the regions of s-d hybridization. If these contributions are small compared with those from the spherelike volumes centered around Γ, we see from Table I that the DD calculations give about 0.35 itinerant d electrons per atom, or again about 5% of the d electrons are itinerant. The effective mass of the itinerant d's in the central spheres from the DD calculation is about twice the free-electron mass.

Figure 3 shows the Fermi surface as deduced from de Haas–van Alphen (dHvA) measurements by Gold *et al.*[11] The central spherelike surfaces arise from the paraboliclike d bands and are to be identified with itinerant d's. In Table I we have

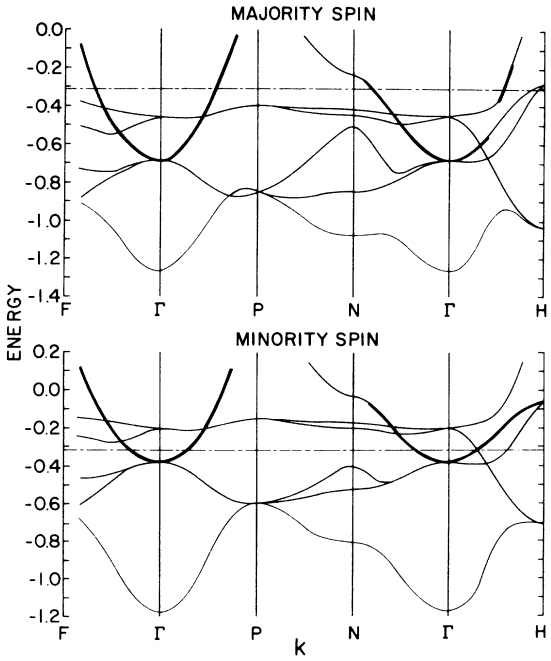

FIG. 2. Band structure of Fe by Duff and Das (Ref. 10). Near Γ the bottom band is due to s-like electrons. The higher five bands are due to d-like electrons.

TABLE I. k_F values for the paraboliclike d bands of Fe (in units of $2\pi/a$).

	Calc.			Expt.	
	Γ-N,F	Γ-P,D	Γ-H	Γ-N	(111)
Majority Spin	0.55	0.50	0.56	0.47	0.46
Minority Spin	0.24	0.27	0.30	0.18	0.18
$n\uparrow$		0.3		0.21	
$n\downarrow$		0.05		0.01	

also listed the measured k_F values of Gold *et al.* of the central spherelike surfaces. If there were no s-d hybridization we would expect the Fermi surface of the s-like electrons to look much like that of Cu, i.e., a spherical-like surface which touches the Brillouin zone at the nearest face (at N for a bcc lattice). However, when both s- and d-type bands cross the Fermi level and are hybridized, the Fermi surfaces become very complex and break up into small regions of electron and hole pockets. This is manifested by the hole surfaces near H (see Fig. 3) and the electron lenses along the axes for the minority spins. The number of itinerant d-like electrons from the s-d hybridized regions is difficult to estimate but it is probably no larger than the number in the central spherelike regions of k space. The number of d electrons in the spheres centered around Γ is 0.21 majority and 0.01 minority spins. So the dHvA measurement also show about 5% or less d electrons in itinerant states. The good agreement between the k_F values for itinerant d electrons from the dHvA measurement and the estimate from the itinerant d's CEP curve may be quite fortuitous or it may be an indication that the shape of the RKKY-type oscillations is not very sensitive to the polarization or details of the itinerant d's wave function near the nucleus. Thus we see that the band calculations and measured Fermi surface do indeed support the picture that the ferromagnetism in Fe arises from the indirect coupling of localized d electrons through about 5% of the d electrons in itinerant d bands. The model indicates a remarkably simple nearly-free-electron behavior of the itinerant d-like electrons which has been so successful for depicting the conduction electrons in nontransition-metal elements. An interesting result is that Fe appears to be just barely ferromagnetic. If k_F for the itinerant d's were much greater it would be antiferromagnetic. This seems to rule out a purely itinerant d-band picture.

As we shall see later in Sec. III the hyperfine-field data for dilute alloys of Co and Ni indicate that the s-like CEP curves in Co and Ni are similar to that of Fe. The estimates of the k_F values of the itinerant d-like electrons needed to produce ferromagnetism from the d-electron CEP curve

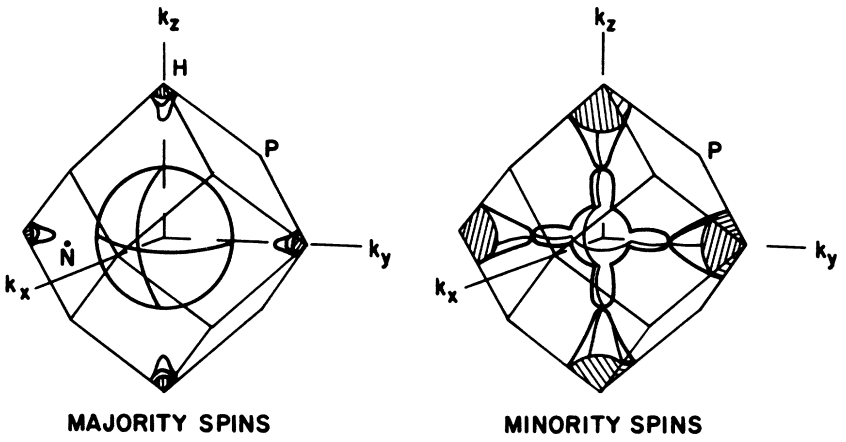

FIG. 3. Fermi surfaces for Fe as deduced from the dHvA measurements of Gold *et al.* (Ref. 11) and band-structure calculations of Refs. 9 and 10. The electron and hole pockets also exist along the k_x axis but have been left out for clarity. There may be more structure near the Brillouin edges which has not been seen yet experimentally.

are about the same as for Fe. For Ni the band-structure calculations[20] give bands which are very similar in appearance to those of Fe except now the majority bands are full and do not cross the Fermi level except in the s-d-hybridized regions. The minority bands appear to hybridize with the s band before any clearly identifiable d bands cross the Fermi level. Therefore the k_F values where a paraboliclike d band crosses the Fermi level are obscured (see Fig. 4 of Ref. 20), and so no reliable estimates of k_F are possible. However, from the similarity of the band structure to that of Fe it seems reasonable that the number of itinerant d-like electrons is again less than about 0.4 electrons/atom. It is often claimed that Co and Ni are itinerant-electron ferromagnets,[1] i.e., that all of the d electrons are itinerant. However, the usual arguments given to support this contention really only require a small degree of itinerancy. The arguments cited by Herring[1] for itinerancy are as follows.

(i) The size of the electronic specific heat shows *some* of the 3d electrons are itinerant. For Fe, Co, and Ni the specific heat is larger than that expected from just the 4s conduction electrons. However, it is known that there may also be magnetic contributions with a linear temperature dependence in the specific heat (at least in alloys) so that it has not been possible to obtain a reliable density-of-states interpretation from the specific-heat data.[21] Thus, how much itinerancy is indicated by these measurements is not known. However, not many itinerant d electrons are required and the model proposed here appears to give enough increase in density of states from the itinerant d electrons (see Fig. 4) to be in agreement with the specific-heat measurements.

(ii) The nonintegral values of the saturation moments are attributed to itinerant d's. This requires at most about 0.5 electrons/atom, which is consistent with the degree of itinerancy proposed here.

(iii) For Co and Ni there is a slight nonequality of the high-temperature moment and the saturation moment.[16] A measure of the localization is indicated by the ratio q_c/q_s, where q_c is the number of magnetic carriers per atom deduced from the Curie-Weiss constant and q_s is the number of carriers deduced from the saturation moment ($=2S$). For a localized moment $q_c/q_s=1$, whereas for the most nonlocal material listed by Rhodes and Wohlfarth (Pt+1-at.% Fe) this quantity is 8.6. For Fe, Co, and Ni the values of q_c/q_s are 1.05, 1.34, and 1.46, respectively, which does not indicate very much itinerancy. Furthermore, by this type of criteria we would expect Ni to appear to be the most itinerant of the three ferromagnetics. Since all three elements have about the same number of itinerant d electrons per atom and Ni has the smallest moment a greater fraction of the Ni moment would

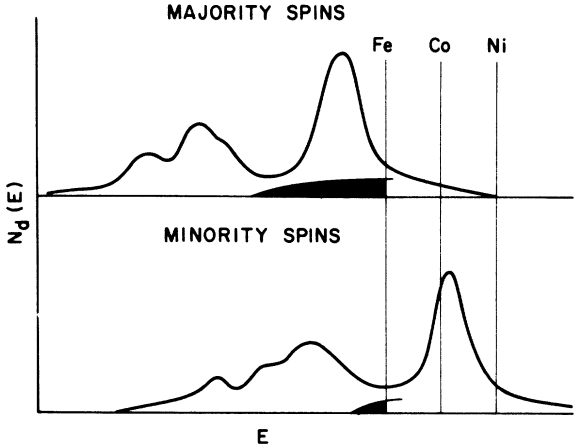

FIG. 4. Sketch of total density-of-states curves of majority and minority spins for Fe, Co, and Ni. The Fermi levels for Fe, Co, and Ni are depicted by the vertical lines. We have also indicated the density of states for the itinerate d electrons by the darkened area.

arise from the itinerant d's.

(iv) Transport phenomena, in particular, thermoelectric-power and high-field Hall and magnetoresistance[22] effects, indicate that some itinerant d electrons are required. The effects observed in the latter two experiments are entirely consistent with the Fermi surfaces depicted in Fig. 3. The hole and electron structures along the axes of the minority spins support open orbits as have been reported in Ref. 22. Thus all the data indicating itinerant d-like electrons in Co and Ni are consistent with the model given here for the origin of ferromagnetism of Fe, Co, and Ni and require only about 5% itinerant d's.

The model proposed here is also consistent with the systematic behavior across the $3d$ transition-metal series. On the left-hand side of the $3d$ transition series the $3d$ electrons are bound as loosely as the $4s$ electrons. Then as the nuclear charge increases the $3d$ electrons become more tightly bound. At some region in the $3d$ series some $3d$-like electrons begin to become localized, i.e., between Cr and Mn. As the nuclear charge increases further a larger fraction become localized. Thus the $3d$ bandwidth becomes narrower per electron as the nuclear charge increases. This is in agreement with band calculations. Ni appears to have about nine of its d bands sufficiently narrow to be considered localized while Fe has about eight localized d bands. Since the ground state of α-Mn is antiferromagnetic[23] we infer that it has a larger number of itinerant d-electrons than Fe. (We shall see that in Fe, Co, and Ni the s-like CEP curve appears to be quite independent of crystal structure and so the complex structure of α-Mn is probably not very important.) Cr has been shown to have entirely itinerant $3d$ electrons.[1(a),24] All the elements to the left of Cr are believed to also have only itinerant d electrons.

B. Comparison of "95% Local Model" with Completely Itinerant Model

Let us discuss the differences between the model proposed here (95% local model) and the model proposed by Friedel *et al.*[12] (itinerant model). They also attributed the magnetic coupling in the transition metals to itinerant d electrons through RKKY-type oscillations. The basic difference is that they assumed all the d electrons were itinerant and then obtained a "localized" magnetic moment by a bootstrapping-type mechanism where the moments are built up by a piling up of electronic charge of one spin, compensated by an equal local repulsion of electrons with the opposite spin. This leads to the RKKY-type oscillating polarization curve. The condition to obtain these local moments is a high density of states at the Fermi level, thus the need for a large number of itinerant d electrons. (In the 95% local model the local moments arise because of the natural tighter binding of the d electrons as the nuclear charge increases.) For the itinerant model the extent of the central portion of the polarization curve (to the first node) was estimated to be at least of atomic size and to depend on the average wavelength of electrons (or holes) in the band. The relevant number to obtain the average wavelength was taken to be the number of holes in the d band. In order to obtain ferromagnetism the extent of the central portion of the localized moment for Fe was then taken to be equal to the interatomic spacing. For Ni the moment extent was found to be 2.5 times the interatomic spacing. These results were directly contradicted by subsequent measurements of the localized-moment distribution by neutron scattering experiments,[15] where a much smaller spacial extent close to that of the free atom (~ 0.4 Å) was obtained. As has been found in the 95% local model, the number of itinerant electrons needed to make the first node of an RKKY-like polarization curve fall beyond the interatomic distance is less than about 0.4 electrons in a band.

C. Variation of Saturation Moment with Alloying—Simple Behavior of Hyperfine Fields at Fe Atoms in Fe Alloys

In order to understand the behavior of the hyperfine fields in dilute alloys of Fe, Co, and Ni let us consider the variation of the saturation moment with alloying. Using the band-structure curves for Fe we can understand the gross features of the variation of the saturation moment of random alloys of Fe, Co, and Ni with nontransition series elements. DD[10] have calculated a density-of-states histogram for majority and minority spins from their band-structure curves. It is very similar to many previous density-of-states curves for Fe. We show a rough sketch of the type of behavior they obtained for the density of states of the $3d$ electrons in Fig. 4. For these considerations a rigid-band approximation (specifically that the shape of the d-band density-of-states curves remains constant and only the Fermi-level position shifts upon alloying) is adequate so we assume the main difference between Fe, Co, and Ni is only the position of the Fermi levels. We have indicated the Fermi-level positions by the vertical lines in Fig. 4. The splitting between the majority and minority spins is of course somewhat different for Fe, Co, and Ni but we have ignored this in Fig. 4. The d bands have a much greater density of states near the Fermi level than the valence ns and np bands. Thus, upon alloying, the excess electrons introduced into the lattice go mainly into the d bands. The number of excess electrons is usually expressed by ΔZ, where Z for Fe is about one and for the solute atom it is the number of valence electrons, i.e., the

value of its column in the Periodic Table, e.g., $Z=3$ and 4, respectively, for Al and Si; thus $\Delta Z = 2$ for Al and 3 for Si. Fortuitously, as indicated in Fig. 4, the Fermi level for Fe falls at a position such that $N_d(E)$ is about the same for both type spins. Therefore, adding nontransition elements to Fe in small amounts increases the number of spin-up and spin-down electrons about equally and the net moment per Fe atom doesn't change.[25] We thus get simple dilution which is well known to occur for alloys[26] of Fe with nontransition elements.

On the other hand, for Ni the Fermi level is known to occur at a position such that the majority d bands are full and the minority-spin bands have about 0.5 hole/atom. Thus, as already described by Mott[27] in 1935, upon alloying with nontransition solute atoms the excess ΔZ electrons go into a minority-spin band and the change in the moment per solute atom is proportional to ΔZ. As is well known, this occurs in Ni alloys[26] with Z for Ni being about 0.5. Since Co also has almost a full majority-spin band and a large density of states for the minority-spin band (see Fig. 4), we expect its alloys to behave similarily to the Ni alloys. Few reliable measurements of the saturation magnetization of alloys of Co with nontransition metals have been made[26] but the few that have been measured behave much more like Ni alloys than like Fe alloys.

Thus we can understand why Fe is ideal to use as a host for measuring the CEP curve and why the nontransition elements cause essentially the same hyperfine-field shifts at nearest-neighbor Fe atoms.[28] The solute atoms do not change the difference in populations of the up and down spins enough to cause moment perturbations on the surrounding Fe atoms and thus they look only like holes in the Fe lattice. We would expect a very different behavior for Ni alloys since upon alloying we increase the number of spin-down d electrons and the number of spin-up d electrons remain fixed. The rigid-band picture of course only gives the average behavior; in reality we expect local fluctuations around the solute atom and thus that the Ni moments surrounding a solute atom would be appreciably perturbed. Such moment perturbations will be discussed at length in a forthcoming paper.

D. Density of States at the Fermi Level

Having only about 5% itinerant d's, as opposed to considering all the d electrons itinerant, can of course have profound effects on quantities that depend on the density of states at the Fermi level. For instance, in the analysis usually given for specific heat, resistivity measurements, and the polarization of electrons at the Fermi level of the $3d$ transition series, all the d's are assumed to be itinerant and the density of states is taken to be the total density of states for the d electrons. We see from Fig. 2 that the itinerant d's do not occur over the whole energy range of the d states, but partially have a behavior typical of a parabolic band which does not extend too far below the Fermi level. The density-of-states behavior expected for the itinerant d's in Fe from the DD calculations is indicated in Fig. 4 by darkened areas. Thus it looks like the localized and itinerant d's may have about equal density of states at the Fermi surface of Fe. In particular we see that the itinerant d density of states does not necessarily follow the total density-of-states curve. For Co, for example, we would expect that at the Fermi level the density of states for the minority spins would be much greater for the localized electrons than for the itinerant electrons. There is also some itinerant d character in the s-d–hybridized part of the Fermi surface that must be considered. Of course for transition elements with no localized states, like Cr, the itinerant d's density of states and the total density of states are the same.

It is of interest to speculate briefly on the polarization of the electrons at the Fermi surface. This quantity has been measured by many experimental techniques.[29] For Fe a polarization of about 50% spin up was measured. An upper limit of this polarization can be estimated by considering only the central spherelike regions near Γ in Fig. 3. The dHvA data would predict a polarization of $[(k_F^{\uparrow})^2 - (k_F^{\downarrow})^2]/[(k_F^{\uparrow})^2 + (k_F^{\downarrow})^2] \sim 0.74$. Since we also have polarized s and d electrons from the hybridized portions of the Fermi surface, the polarization would be expected to be less than 0.74, but greater than 0.34, which would be obtained by including one unhybridized and unpolarized $4s$ electron in the above estimate. For Ni the experimental situation is very controversial and appears to depend strongly on the crystallographic direction. Owing to the more dominant nature of the s-d hybridized electrons in Ni, it is reasonable to expect more dependence of the polarization on the crystallographic direction in Ni than in Fe and difficult to estimate what the net polarization on a polycrystalline sample should be.

E. Spin-Wave Spectra of Fe and Ni

Recently the spin wave spectra of Fe and Ni have been measured by neutron scattering experiments.[30] For Fe the spin-wave intensity is seen to drop rapidly around 90 meV, corresponding to a wave-vector change q of about 0.65 Å^{-1}, depending slightly on the crystallographic direction. The excitations which compete with the magnons are spin-flip excitations (Stoner excitations) with ~90 meV of the Fermi level. Interpreting this in terms of the model presented here we can see from the band structure shown in Fig. 2 that the dominant excita-

tions of this type are from the spin-up to spin-down (or vice versa) spherelike itinerant d Fermi surfaces centered around Γ. From Table I we see that the dHvA measurements show this q value to be $k_F^{\dagger} - k_F^{\downarrow} \simeq 0.285\ (2\pi/a) = 0.63\ \text{Å}^{-1}$, in excellent agreement with the measured value. It appears that this type of measurement may be one of the most accurate ways to measure the directional dependence of the k_F differences of the spherelike surfaces centered at Γ. Thus the behavior of the spin-wave spectrum of Fe supports the interpretation that the spherelike surfaces are to be associated with rather pure itinerant d-electron states.

For Ni similar spin-wave intensity decreases are seen at $\simeq 90$ meV, which corresponds to $q \simeq 0.45\ \text{Å}^{-1}$. An interpretation similar to that for Fe should apply but unfortunately since for Ni the s-d hybridization plays a dominant role and the Fermi surface structure is not as well established as for Fe, it is difficult to identify the spin-flip excitations which are competing with the magnons. None of the recent band calculations lead to much success in such attempts.[31]

III. MODEL FOR THE ORIGIN OF THE HYPERFINE FIELDS

For the past decade experimentalists have been measuring values of hyperfine fields at the solute atom in Fe, Co, and Ni by Mössbauer, NMR, and perturbed-angular-correlation (PAC) techniques.[32] An up-to-date tabulation of the data is given in columns 3–5 in Table II. Here we list the measured hyperfine-field values at the lowest temperature measured. See Ref. 32 for these temperatures and the individual references for data appearing in 1968 or before. Later data are referenced at the end of Table II. Where no sign is indicated it has not been measured. In keeping with the usual procedure we have listed the measured values in columns 3–5.

The true hyperfine-field values H_Z^{hf} are given by

$$H_Z = H_Z^{hf} - DM + \tfrac{4}{3}\pi M + H_d \ , \qquad (1)$$

where D is the demagnetizing factor, M is the magnetization, and H_d is the dipole sum taken over a sphere surrounding the solute atom. For cubic symmetry H_d is zero. In practically all measurements either foils are used or, in the case of NMR, the domain-wall signal is observed; so $D = 0$. Thus the quantity $\frac{4}{3}\pi M$ should be subtracted from the values in columns 3–5 to get the true hyperfine-field values. This has been done in obtaining the values listed in columns 8 and 10, and elsewhere as noted. The values of $\frac{4}{3}\pi M_s$ are 7, 6, and 2 kG, respectively, for Fe, Co, and Ni.

The data taken by Mössbauer and NMR techniques are usually quite reliable. However, that

TABLE II. Hyperfine fields at solute atoms in Fe, Co, and Ni (all fields in kG except H_{ns}^Z).

1 Z	2 Element	3 H_z^{Fe}	4 H_z^{Co}	5 H_z^{Ni}	6 H_{ns}^Z(MG)	7 $-H_C^Z$ in Fe	8 H_v^Z in Fe	9 V_z[a]	10 H_v^Z/H_{ns}^Z	11 P_v
13	Al	−55(1)	32(1)		0.5					
18[b]	Ar[c]			280(23)				23.9		
20[d]	Ca[c]	−100(9)	−70(15)	<30	0.8	260	−40	25.9		
21	Sc	58			1.0	272	+(7–123)	18	0.007–0.12	0.08
23	V	−87	48(1)	7.5(2)	1.4	102	8	8.5	0.005	0.006
25	Mn	227	140	325(1)	1.8	130	↑	7.39		
26	Fe	−339	−323	283(3)	2.0	145		7.1		
27	Co	−288	−216	−120(1)	2.2	160	moment	6.6		
28	Ni	234	188	75	2.4	174	↓	6.59		
29	Cu	−213	157	−47	2.6	188		7.09		
30[e]	Zn[c]	−105(35)			3.0	218	106(35)	9.17	0.035	0.018
31	Ga	110(3)	62(1)		4.0	290	393	11.8	0.10	0.035
33[f]	As[c]	+319(33)	+249(28)	+88(10)	7.5	544	856	13.1	0.11	0.031
33[g]		+145(18)					682		0.09	
36[h]	Kr	1500			13	942	2440	27.82	0.19	0.18
39	Y	+286(5)			2.4	174	453	16.1	0.19	0.06
40	Zr		90(2)		2.6	188		14.0		0.04
41	Nb	−258	−187[i]	−41(1)	2.9	210	↑	10.8		
42	Mo	−265(5)	150(3)		3.3	239		9.4		
43[e]	Tc[c]	−400(160)			3.7	268				
		−320(65)					moment			
44	Ru	−500(10)	415(16)	−217[c](5)	4.0	290	↓	8.3		
45	Rh	−550(10)	392(8)	210	4.4	319		8.27		
46[i]	Pd	−530	−357	−173	4.8	348		8.89		
47[j]	Ag	−447(2)		−122(4)	5.2	377		10.28		
48	Cd[c]	−348(10)		−69(15)	6.4	464	109	13.0	0.017	0.03

TABLE II. (*Continued*)

1 Z	2 Element	3 H_z^{Fe}	4 H_z^{Co}	5 H_z^{Ni}	6 H_{ns}^Z(MG)	7 $-H_L^Z$ in Fe	8 H_v^Z in Fe	9 V_z[a]	10 H_v^Z/H_{ns}^Z	11 P_v
49	In	−288(6)		−33(1)	9.1	660	365	15.7	0.040	0.057
50	Sn	−81(4)	−20(15)	+18(10)	12	870	782	16.2	0.065	0.062
51	Sb	+230	187(4)	+94(2)	~15	1088	1310	18.4	0.087	0.084
52	Te	+620(20)	550(50)	+195(10)	~20	1450	2060	20.5	0.10	0.10
53	I	1170(16)			19	1377	2540	25.7	0.13	0.16
54[k]	Xe[c]	1400(200)			22	1595	2990	36.81	0.14	0.27
55[l]	Cs	273(10)			2.4	174	440	70	0.18	0.60
56[m]	Ba[c]	−85(14)			3.0	218	126	39	0.042	0.29
72	Hf	−300(60)*			7.7	558	250	15.7	0.033	0.057
72[n]		606(70)					−55(70)			
73	Ta	−656(13)		−98(2)	8.3	602		10.9		
74	W	−643(13)	−388(8)	−90(25)	9.3	674	24	9.53	0.003	
75	Re	−660(15)	491[i]	−100(2)	10.8	783	16	9.3	0.0015	
76	Os	1130(23)	870(17)	300(6)	12.3	892	↑	8.46		
77[o]	Ir	−1395(16)	965(19)	−467(3)	13.9	995	moment	8.58		
78	Pt	−1280(26)	830(17)	−340(7)	16.0	1160	↓	9.10		
79	Au	−1280(26)	−797(16)	−294(6)	18.5	1340	50	10.2	0.003	0.002
80[p]	Hg[c]	−440(105)	−370(78)	−86(22)	21.5	1560	1110	14.8	0.052	0.048
81[p]	Tl[c]	−185(70)	−90(35)		26	1885	1690	17.24	0.065	0.072
82[q]	^{207}Pb[c]	+660(45)	+430(32)	+115(15)	33	2392	3050	18.27	0.092	0.083
	^{208}Pb[c]	+280(70)	+280(70)	125(35)			2670		0.081	
82[r]	^{204}Pb[c]	+262(5)					2650		0.080	
83[r]	Bi[c]	1180(130)		325(35)	42	3045	4220	21.3	0.10	0.11
83[s]				+160(30)						
83[t]		800−1000		390(15)						
86[u]	Rn[c]	~+900			~60	4350	5250	42.0	0.088	0.40
88[u]	Ra[c]	~−220			4.7	341	114	36.5	0.024	0.35
88[v]		−120(25)	−100(30)	−30(18)			214		0.046	
90[w]	Th[c]	−310(60)			5.5	399	82	20.2	0.015	0.10

[a]Atomic weight divided by the density (Ref. 40). The conversion factor from V to the atomic radius is $0.736V^{1/3}$.

[b]H. G. Devare and H. de Waard, Phys. Rev. B 5, 134 (1972).

[c]Perturbed angular correlation data.

[d]M. Marmor, S. Cochavi, and D. B. Fossan, Phys. Rev. Lett. 25, 1033 (1970).

[e]P. Inia, Y. K. Agarwal, and H. de Waard, Phys. Rev. 188, 605 (1969). Also Tc in Fe of -320 ± 65 kOe by E. Gerdan *et al.* (private communication).

[f]R. C. Chopra and P. N. Tandon (unpublished).

[g]A. J. Becker and F. C. Zawislak, International Conference on Angular Correlations in Nuclear Disintegrations, Delft, 1970 (unpublished). Referenced in f.

[h]Provisional value obtained by Kolk. Private communication by H. de Waard.

[i]More recent values by M. Kontani and J. Itok than given in J. Phys. Soc. Jap. 22, 345 (1967).

[j]R. A. Fox, P. D. Johnston, and N. J. Stone, Phys. Lett. A 34, 211 (1971).

[k]L. Niesen, thesis (Leiden, 1971) (unpublished). Communicated by H. de Waard.

[l]H. de Waard and S. A. Drentge, Proc. R. Soc. Lond. A 311, 139 (1969).

[m]H. W. Kugel, T. Polga, R. Kalish, and R. R. Borchers, Phys. Lett. B 32, 463 (1970). Uncertain value due to lack of knowledge of g factor.

[n]P. Steiner, E. Gerdan, and D. Steenken, Proc. R. Soc. Lond. A 311, 177 (1969). This value is claimed to be more reliable than the PAC value.

[o]In Fe, C. J. Perlow, W. Henning, D. Olsen, and G. L. Goodman, Phys. Rev. Lett. 23, 680 (1969); In Ni, G. Eksa, E. Hagn, T. Butz, and P. Kienle, Phys. Lett. B 36, 328 (1971).

[p]F. C. Zawislak, D. D. Cook, and M. Levanoni, Phys. Lett. B 30, 541 (1969). Shows value for Pb.

[q]J. D. Bowman and F. C. Zawislak, Nucl. Phys. A 138, 90 (1969). The earlier value of +262 kG was again obtained in r.

[r]F. Bacon, H. Haas, G. Kaindl, and H. E. Mahnke, Phys. Lett. A 38, 401 (1972).

[s]F. C. Zawislak and D. D. Cook, Bull. Am. Phys. Soc. 14, 1171 (1969).

[t]M. Kaplan, P. D. Johnstone, P. Kittel, and N. J. Stone, Phys. Lett. A 41, 315 (1972).

[u]E. J. Ansaldo, L. Grodzins, and R. Kalish, Phys. Lett. B 30, 538 (1969). Inaccurate since g factor is not well known.

[v]I. Plesser, M. Levanoni, and F. Zawislak, Bull. Am. Phys. Soc. 14, 1171 (1969).

[w]E. J. Ansaldo and L. Grodzins, Phys. Lett. B 34, 43 (1971). Values are probably smaller than true values.

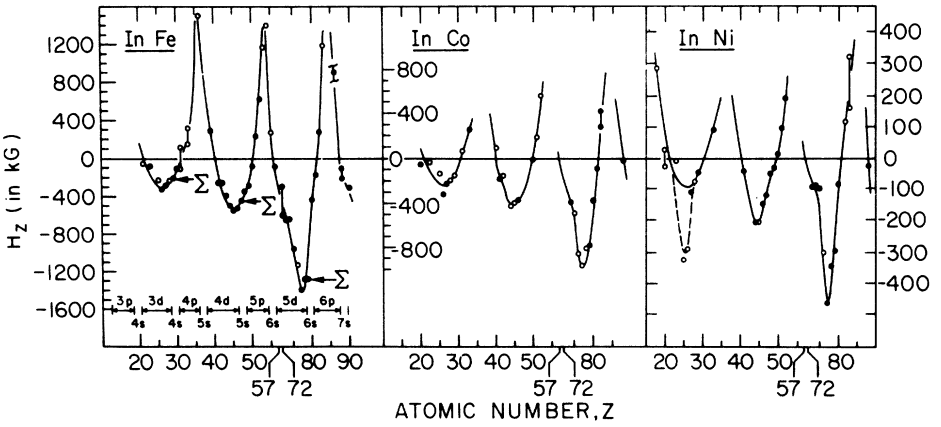

FIG. 5. Solute-atom hyperfine field variation with atomic number Z for Fe, Co, and Ni matrices. The ordinates are scaled proportional to the host moments. ●, sign measured; ○, sign not measured.

taken by PAC techniques is often unreliable, owing to the difficulty of knowing the environment of the emitting nucleus; it should really be supplemented by channeling experiments. This has been done in some cases. Therefore, in Table II the data taken by PAC are denoted by a superscript c and as can be seen different workers often obtain different values by this method. In these cases we have listed all the different values. The values for solute atoms of $Z > 82$ are especially in doubt. The values of the hyperfine fields at solute atoms in Fe, Co, and Ni are shown plotted in Fig. 5. As is well known these data show two overwhelmingly simple features: namely, the hyperfine field as a function of Z shows a regular systematic variation with Z and the field at a given solute atom in the three hosts is very nearly proportional to the host moment. This can be seen clearly in Fig. 5, where the ordinates are plotted on scales proportion to the moments and thus the plots for Fe, Co, and Ni look very similar. We can explain this observed behavior with a model which attributes the total hyperfine field at any solute atom to three distinct contributions.

Thus a general model for the hyperfine field at an atom of atomic number Z in a dilute alloy with these ferromagnetic metals (assuming no orbital momentum contribution to the hyperfine field) can be considered to be composed of three contributions:

$$H_Z = H_{cp}^Z + H_{ce}^Z + H_v^Z \ , \qquad (2)$$

where H_{cp} is due to the polarization of inner core $1s$, $2s$, and $3s$ electrons by the magnetic electrons.

H_{ce} is due to the polarization of the $4s$-like conduction electrons by the moment on the transition metal atoms; the d-like itinerant electrons of course have zero probability of being at the nucleus and therefore do not contribute to the hyperfine field. This oscillatory CEP has been measured for Fe and is reliably known out to N_6. We will comment here on the values used in this analysis; they are listed in Table III. Originally, measurements[6] of the hyperfine-field shifts of the various neighbor shells due to substituting Al or Si for an Fe atom in dilute Fe alloys were made using the Mössbauer technique. A careful computer analysis of these spectra indicated that the spectra had sensitivity to about four parameters. The parameters used in this analysis were the shifts of the first four or five neighbor shells and additivity of shifts was assumed. The computer generated contour error maps [Fig. 4 in Ref. 6(b)] which indicated the quality of fit by the mean-square deviation (MSD). We found that there was often another minimum in the MSD when the assignment of shifts due to different neighbor shells was interchanged. A solution of the type (N_2 negative and N_3 positive) like that given in Fig. 1 was best but the next best solution had N_2 small and positive and N_3 negative. At that time we decided that straightforward Mössbauer spectra of this sort could yield no better shift values or sensitivity since the analysis left out certain features that surely exist, e.g., dipolar structure due to removing cubic symmetry by introducing a solute atom and magnetic shielding or saturation effects[7]

TABLE III. Measured values of the hyperfine field contributions per Fe atom; ΔH_i from the various neighbor shells, Ref. 7 (in kG).

Shell	Ni	ΔH_i
1	8	−27.1
2	6	−6.1
3	12	+5.4
4	24	+1.4
5	8	+0.7
6	6	+1.4

$$H_{\Sigma}^{Fe} = \sum_{i=1}^{6} N_i \Delta H_i = -145 \text{ kG}$$

that remove additivity. The hyperfine spectra of the dilute alloys was next measured using pulsed-NMR techniques whose resolution is inherently about 10 times better[33] than the Mössbauer technique. Unfortunately the second- and third-neighbor shifts are so small that even with a computer analysis the uncertainties due to the dipolar shifts and nonadditivity still made it inconclusive as to whether N_2 was negative and N_3 positive or vice versa, although again N_2 negative and N_3 positive was the preferred solution in the computer analysis. However, other authors[34] preferred the "inverted" solution, although none of these authors carried out a computer analysis which evaluated the relative "goodness of fit" of the various solutions. The difficulty with the dilute alloys is that there are too many parameters involved to obtain an unambiguously convincing solution. For example, the number of parameters becomes prohibitive if one wants to obtain the shifts due to the six-nearest-neighbor shells and has structure of the same order as many of the shifts due to dipolar and nonadditivity effects. Thus we decided to look at the ordered alloy system (Fe_3Si) more carefully since here we have three very different type sites, each of which is affected by only two of the first six neighbor shells. With this system we have good enough sensitivity to be able to measure directly the dipolar shifts and the nonadditivity effects. The only question is, does this system behave in a way such that the results can be extrapolated back to pure Fe. Many types of measurements [see Refs. 6(b) and 7(a)] indicate that the CEP does indeed behave similarly to that of pure Fe and so we feel confident that the shifts measured in the Fe_3Si system, especially for shells of N_3 and further out, are similar to those of pure Fe. The N_2 and N_3 shifts are seen to be unambiguously negative and positive, respectively, with the latter being of exactly the same value as obtained from the dilute alloys. Furthermore we will see later that the sum of the shifts due to the inverted solution gives an unreasonably high value for the CEP owing to the surrounding neighbors.

The measured oscillatory polarization may arise from: an RKKY-type[4] indirect exchange interaction between the magnetic ions and the 4s-like conduction electrons; some s-d interband mixing and hybridization[35]; and a charge perturbation[36] contribution. In Ref. 7(b) we concluded that the charge-perturbation contribution was small and indicated that the interband mixing and indirect contributions may be comparable. In recent work[37] it was suggested that the polarization due to the spin and charge perturbations may be of comparable magnitudes, but as pointed out by Gunnarson *et al.*[38] these calculations neglect correlations between electrons, and when these are included the dielectric response effects are reduced considerably. Furthermore, if the polarization were mainly due to a charge-perturbation effect we would expect the shifts to be dependent on the ΔZ, as originally predicted in Ref. 36 and also implied in Ref. 37. Since no such dependence occurs and is not expected to occur in Fe alloys for a moment-dependent perturbation as discussed in Sec. II B we believe the main effect is due to a moment perturbation. However, in any case, in this section the origins of the spin-density oscillations will not affect the conclusions since we use only the measured values in the analysis. It is convenient to divide the H_{ce} term into two parts:

$$H_{ce} = H_s + H_\Sigma \ , \tag{3}$$

where H_s is the field due to the s-like CEP from the moment on the solute atom itself and H_Σ is the field due to the 4s polarization at the solute atom from the moments of all the surrounding host atoms. For Fe $H_\Sigma^{Fe} = \sum_{i=1} N_i \Delta H_i$, where N_i is the number of atoms in the ith neighbor shell and ΔH_i is a hyperfine field due to the CEP from an Fe atom in the ith shell. The ΔH_i values are listed in Table III.

H_v is a positive field due to the valence ns-like electrons which remain near the solute ion shielding the excess charge. When the volume of the solute atom is larger than the volume available upon removing a host atom, the ns-like valence electrons overlap with the host matrix and become positively polarized by an amount proportional to the volume misfit of the solute atom. This term was evaluated and discussed in Refs. 7(b) and 39, but there is more data available now so we will update that discussion in Sec. IV.

Each of the three contributions dominates at different regions of the Periodic Table. We can easily see where each term is dominant by considering a plot of the atomic volume as a function of Z, as shown in Fig. 6. These values are also listed in column 9 of Table II. Here the volumes are given in units of atomic weight divided by density[40] on the left-hand scale. The equivalent spherical atomic radii cubed are given on the right-hand scale in Å^3. We will see that the volume available for a solute atom upon removal of an Fe atom from an Fe lattice is 10 (in units of the left-hand scale). Thus the field at the solute atoms with volumes greater than 10 soon become dominated by the positive H_v term and the general shape of the hyperfine-field curves in Fig. 5 is very similar to the atomic volume curve of Fig. 6. In the regions near the latter part of any d transition series (see the Fe curves in Fig. 5) the d transition-series solute atoms tend to develop a moment. Thus in these regions the H_{cp} term may become dominant. There are also solute atoms which develop no moment

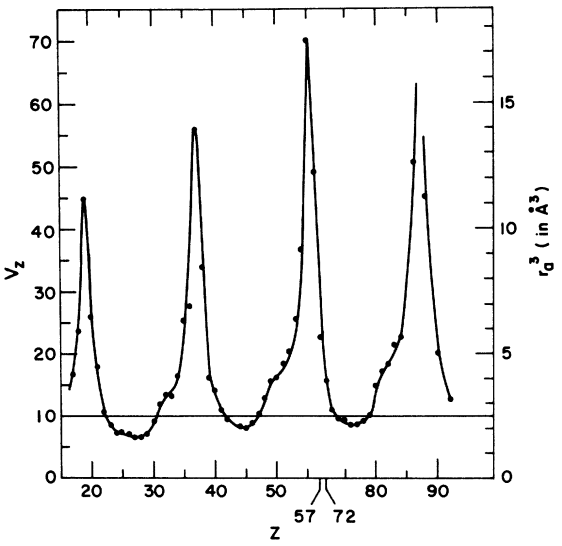

FIG. 6. Variation of atomic volume with atomic number. Left-hand scale is the atomic weight divided by the atomic volume. The right-hand scale is the atomic radius cubed in Å^3. The conversion factor is $r_a = 0.736 V_z^{1/3}$.

and whose volume is small enough so that they fit into the host matrix with no volume overlap. For these solute atoms, since H_{cp}, H_s, and H_v are all zero, the measured hyperfine field is just H_Σ. These atoms are shown on Fig. 5 by the arrows marked Σ in the Fe data. The hyperfine-field values for these solute atoms are thus of great significance since they are a direct measure of H_Σ^Z. In order to compare these values with the measured value of H_Σ^{Fe} (−145 kG) we need first to determine how each of the hyperfine-field contributions scale with solute atom and host.

a. Scaling of H_{cp}^Z term. For a solute atom of any *nd* transition series, since the series has essentially the same atomic core, H_{cp}^Z will simply be proportional to the moment of the solute atom, i.e.,

$$H_{cp}^Z = \mu_z H_{cp}^{nd} \ , \tag{4}$$

where H_{cp}^{nd} is the hyperfine field per Bohr magneton due to the core *s* electrons of the *nd* transition series. In particular, for solute atoms of the 3*d* transition series referenced to the core polarization of Fe we have

$$H_{cp}^Z = (\mu_z/\mu_{Fe}) H_{cp}^{Fe} \ . \tag{5}$$

b. Scaling of H_v^Z term. Since the hosts Fe, Co, and Ni all have essentially the same atomic volumes (see column 9 of Table II) the overlap of any solute atom in these hosts is about the same. Therefore the polarization of the outer *ns* electrons and thus H_v^Z will just be proportional to the moment of the host, μ_h; thus

$$H_v^{Z\ in\ h} = (\mu_h/\mu_{Fe}) H_v^{Z\ in\ Fe} \ . \tag{6}$$

c. Scaling of H_{ce}^Z term. For solute atoms that develop a moment we see from the similar shapes for the three hosts in Fig. 5 that the hyperfine field is usually proportional to the host moment. There are notable exceptions, however, e.g., Mn and Fe in Ni have especially large hyperfine fields, but these do not concern us here. The majority of solute atoms do not develop a moment and for these Eq. (1) becomes simply

$$H_z = H_\Sigma^Z + H_v^Z \ .$$

For these solute atoms H_z is indeed observed to be proportional to the host moment in very dilute alloys (see Fig. 5). However, now two possible expressions for H_Σ^Z arise. Since H_v^Z is proportional to the host (Fe, Co, or Ni) moment this means H_Σ^Z is also proportional to the host moment. The first possibility that is consistent with the experimental results is that for pure Co and Ni

$$H_\Sigma^{Co,Ni} = (\mu_{Co,Ni}/\mu_{Fe}) H_\Sigma^{Fe} \ . \tag{7a}$$

However, considering any solute atom in a particular host *h*, there is another multiplying factor[7,39] due to the 4*s* electrons taking on the character of the valence *s* electrons of the atom at whose nucleus the hyperfine field is being measured; thus

$$H_\Sigma^{Z\ in\ h} = (H_{ns}^Z/H_{4s}^h) H_\Sigma^h \ , \tag{8}$$

where H_{ns}^Z is the hyperfine coupling constant of atom *Z*; i.e., it is the hyperfine field at a nucleus of atom *Z* due to one polarized *ns* electron. We use the hyperfine coupling constants given in Ref. 32; we found them to be very reliable, as discussed in Ref. 7. These values are listed in column 6 of Table II. Thus in analogy with Eq. (8) we might expect that Eq. (7a) should also include the factor $H_{4s}^{Co,Ni}/H_{4s}^{Fe}$ so that

$$H_\Sigma^{Co,Ni} = (H_{4s}^{Co,Ni}/H_{4s}^{Fe})(\mu_{Co,Ni}/\mu_{Fe}) H_\Sigma^{Fe} \ . \tag{7b}$$

Here we have implicitly assumed that there are an equal number of 4*s* conduction electrons in pure Fe, Co, and Ni, which is not true. Another multiplicative factor could be put in to take this into account. [There is no factor involving the number of *s* conduction electron in Eq. (8), since for very dilute alloys this number is the same for the solute and host atoms.] Since Fe, Co, and Ni all have different structures and numbers of conduction electrons and the experimental data mainly show strong trends and not details to great reliability, we are not justified in assuming that the CEP behavior in Co and Ni is exactly like that in Fe, as is implicit in Eq. (7b). We can only conclude that its behavior is similar to that in Fe as is indicated by Eq. (7a).

A. H_Σ Only Cases

Here we wish to consider those solute atoms whose hyperfine fields come from only the H_Σ

term. From Table II we see that the more accurately measured solute atoms that best fit this category are Cu, Ag, and Au. Using Eq. (8) and the corrected hyperfine-field values at Cu, Ag, and Au [subtracting $(4\pi/3)\,M_s$ from the values in columns 3–5 in Table II] we can obtain values for $H_\Sigma^{\mathrm{Fe,Co,Ni}}$ and compare them to these quantities obtained in other ways. These values are listed in Table IV. Ag and Au may have a small H_v contribution and we have indicated this correction in Table IV. We can compare the H_Σ^{Fe} values directly with that obtained by summing over the measured CEP curve.[7] This gave −145 kG, as listed in the last row in Table IV. We see that this value agrees reasonably well with those obtained from Cu, Ag, and Au in Fe. We can also calculate the values of $H_\Sigma^{\mathrm{Co,Ni}}$ obtained from the CEP curve of Fe using Eqs. (7a) and (7b). These are also listed in the last row of Table IV and again agree well with the $H_\Sigma^{\mathrm{Co,Ni}}$ values obtained from Cu, Ag, and Au. Notice that using Eq. (7a) or (7b) makes little difference since $H_{4s}^{\mathrm{Fe,Co,Ni}}$ are quite similar. This agreement obtained from both types of extrapolation gives an internal consistency check on the model for the origin of the hyperfine field. The value of H_Σ^{Fe} obtained from an "inverted" solution[34] discussed earlier is between −240 and −275 kG and would lead to $H_\Sigma^{\mathrm{Co}} \simeq -220$ kG and $H_\Sigma^{\mathrm{Ni}} \simeq -85$ kG. These do not agree at all well with the values obtained from the H_Σ only cases. This further indicates that the inverted solution is not the correct solution.

The important implication of the scaling of the negative H_Σ values according to Eq. (7) is that the behavior of the CEP curve in all three hosts must be quite similar; i.e., they all have a large negative region around the nearest-neighbor distances. It is not obvious *a priori* that the CEP curves for Co and Ni should be similar to that of Fe since they all have different lattice structures and numbers of 4*s* conduction electrons. But apparently the structures and number of 4*s* conduction electrons are not sufficiently different from Fe to appreciably change the CEP behavior. As we shall see, the similarity of the CEP curves also requires that the moments of all three hosts have a very similar spacial localization.

TABLE IV. $H_\Sigma^{\mathrm{Fe,Co,Ni}}$ obtained from H_Σ only cases (all values in kG).

Element	H_Σ^{Fe}	H_Σ^{Co}	H_Σ^{Ni}
Cu	−169	(−) 138	−45
Ag[a]	−175 to −180		−57 to −59
Au[b]	−139 to −143	−95 to −99	−38 to −40
From CEP Eq. (7a)	−145	−112	−40
curve Eq. (7b)		−123	−48

[a]Ag may have H_v contributions of $H_v^{\mathrm{Fe}} = 15$ kG, $H_v^{\mathrm{Ni}} = 4$ kG.

[b]Au may have H_v contributions of $H_v^{\mathrm{Fe}} = 37$ kG, $H_v^{\mathrm{Co}} = 29$ kG, $H_v^{\mathrm{Ni}} = 10$ kG.

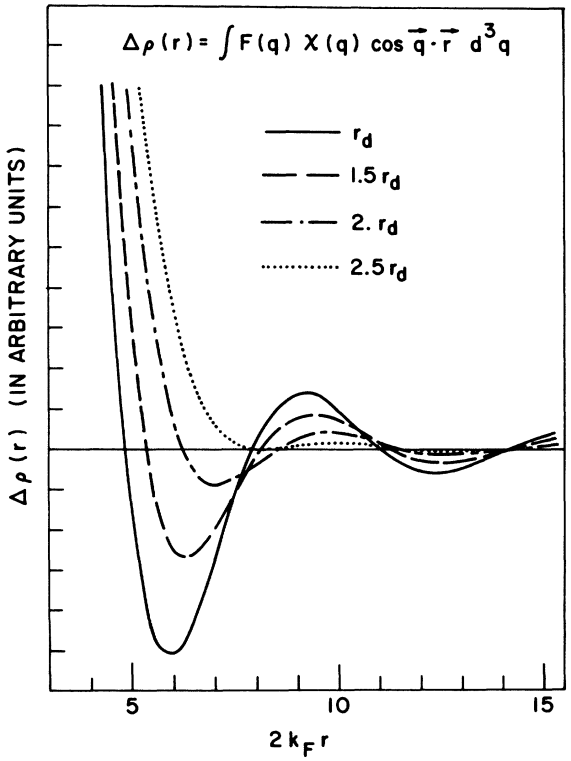

FIG. 7. Dependence of spin-density oscillation upon the extent of the magnetic ion's wave function.

B. Spacial Localization of Co and Ni Moments

We can argue that in order for the CEP curves of Fe, Co, and Ni to have similar shapes and magnitudes per Bohr magneton, as indicated above, the spacial extent of the moments of Fe, Co, and Ni cannot be appreciably different. We represent the 4*s*-like electron spin-density oscillation $\Delta\rho(r)$ by the form-factor representation[41] as

$$\Delta\rho(r) \sim \int F(q)\,\chi_0(q)\cos(\vec{q}\cdot\vec{r})\,d^3q\ , \tag{9}$$

where $F(q)$ is the form factor of the host atoms. $\chi_0(q)$ is the spin susceptibility of a noninteracting electron gas,

$$\chi_0(q) = \chi_p\left[\tfrac{1}{2} + \left((1-x^2)/4x\right)\ln\left|(1+x)/(1-x)\right|\right]\ , \tag{10}$$

where χ_p is the Pauli susceptibility, $x = q/2k_F$, and k_F is the wave vector at the Fermi surface ($\simeq 1.3 \times 10^8$ cm^{-1} corresponding to $n_s \simeq 1$ for Fe). We show the results of such calculations in Fig. 7, where we have used $F(q) = e^{-\beta^2 x^2}$ with the value of β determined from neutron scattering experiments.[15] This value of β corresponds to the radial width r_d of the moment of 3*d* electrons being about

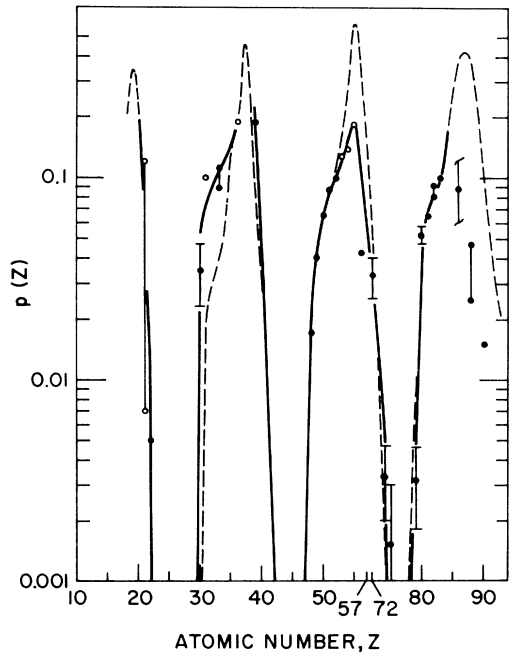

FIG. 8. Polarization at a solute atom due to volume misfit in an Fe matrix as a function of atomic number. The data points and solid curve are the derived polarization, H_v^Z/H_{ns}^Z. The dashed curve is the calculated polarization from the volume-misfit model.

at 0.4 Å. We see from Fig. 7 that an expansion of the 3*d* radial extent by 0.2 Å would decrease the main negative oscillation by about 40%, whereas an increase of width by about 0.6 Å leaves no CEP oscillations. The result that the spacial extents of the moments in Fe, Co, and Ni are very similar was of course already well known from the magnetic-form-factor measurements by neutron scattering experiments,[15] where it was found that the form factors of Fe, Co, and Ni varied by less than 10% and are very similar to those calculated for free atoms. The above argument does not depend on the detailed form of $\chi_0(q)$. The same conclusion can also be reached by considering that a spread out moment would lead to a superposition of a number of oscillating CEP curves of the form shown by the solid curve in Fig. 7, each originating from a region of the spread out moment. Such a superposition of oscillating curves always tends to wash out the oscillations and thus for a wide enough moment spread the oscillations will disappear entirely.

IV. EVALUATION OF THE H_v TERM

We wish here to up-date the data and analysis given in Ref. 7. From Eqs. (1) and (2) we see that for solute atoms that do not develop a moment

$$H_z = H_L^Z + H_v^Z \ .$$

For an Fe matrix, H_L^Z is obtained from Eq. (8),

$$H_L^Z = (H_{ns}^Z/H_{4s}^{Fe})H_L^{Fe} \ .$$

We tabulate the values of $-H_L^Z$ obtained in this way in column 7 of Table II. We then obtain $H_v^Z (= H_z^{Fe} - H_L^Z)$ and tabulate these in column 8 of Table II. Here H_Z^{Fe} has been corrected by subtracting $(4\pi/3)M_s$ from the values in column 3.

We can then obtain the polarization of the outer *ns* valence electrons by dividing H_v^Z by H_{ns}^Z. (This assumes that on the average one excess *ns* electron is left in the vicinity of the solute ion.) These polarizations are tabulated in column 10 of Table II and are plotted in Fig. 8 as the data points. We now wish to compare these derived polarizations with those obtained by the volume-misfit model. Most of the solute atoms have two outer *ns* valence electrons. (We discuss the cases which have only one later.) Let us assume that on the average one of the two *ns* electrons remains near the solute ion participating in the shielding of the excess charge at the solute ion. This *ns* valence electron becomes polarized by an amount proportional to the volume misfit of the solute atom in the Fe matrix, i.e., $V_z - V_0$, where V_0 is the volume available to the solute atom upon removing an Fe atom from the lattice. Thus we have

$$p_v(z) = C(V_Z - V_0) \ . \qquad (11)$$

We evaluate C and V_0 by fitting Eq. (11) to the derived polarization (H_v^{Fe}/H_{ns}^Z) listed in column 10. We find $V_0 = 10$ in the same units as used in column 9. This corresponds to a spherical volume whose radius is $r_0 = 1.58$ Å. In the units corresponding to those in column 9, C is 0.01, which corresponds to a spherical volume with a radius of 3.4 Å. Thus it looks like a hole with a spherical radius of 1.58 Å is available to the solute atom upon removing an Fe atom. If the solute atom had a radius of 3.4 Å its remaining *ns* valence electron would appear to be completely polarized. The C value is somewhat arbitrary since we have assumed that the shielding of the excess charge was done by one *ns* valence electron (any *np* electrons of the solute atom may also participate in the screening but they contribute very little to the hyperfine field). If the average number of shielding *ns* electrons were m then the polarization and C would be changed by a factor of $1/m$.

The values calculated from Eq. (11) are shown as the dashed curve in Fig. 8. We see that this model fits the gross features of the data very well although there are some data that deviate quite a bit from Eq. (11). In particular, the rare gases and alkali metals might be expected to deviate since the outer *ns* electrons of the rare gases are bound rather tightly and the alkali metals only have one outer *ns* valence electron. Thus these values are expected to be low, and are by a factor of 2 or 3.

The other areas of large deviation are near $z = 30$ and $z = 85$ or greater. Most of the values in these regions were determined by PAC methods, where as we have mentioned, the values may be very uncertain owing to the uncertainty of the environment of the decaying nuclear species. The values for $z > 85$ are especially unreliable. However, for the elements in the region $z = 30$–36 we may be observing real deviations from the model for H_v. In particular, the field at As has been measured quite extensively. We see that in this region the polarizations obtained from the experimental data are about a factor of 3 greater than those obtained from the volume-overlap model. It may be that here the d levels of the solute atoms are so close to the Fermi level of the hosts that they cause a resonance state (virtual level) in the $4s$-p bands. This could lead to an enhancement of the $4s$-electron density which is shielding the excess charge on the solute atom and thus an increased H_v term. We should expect some deviation from Eq. (11) due to specific details of the wave functions of the solute atoms since the overlap model is very simple in that it only considers an average atomic radius. Actually the simple volume-overlap polarization fit is quite striking since it represents the gross features very well and occurs over polarizations that vary by more than two orders of magnitude.

The fact that in general the simple overlap model works so well over most of the Periodic Table indicates that effects such as calculated in Refs. 37 and 38, i.e., producing a spin polarization due to an excess charge in a polarized electron gas, are not important. It appears that there is no additional polarization of the host in the region surrounding any solute atom since the H_Σ^z term is obtained by the usual scaling of the H_{ce} term as given by Eq. (8).

The above treatment has only been given for an Fe matrix. A similar treatment for Co and Ni matrices works well also, but as seen in Table II we have much less data available for these hosts.

TABLE V. H_Σ and H_v for Sn and Tl in Fe, Co, and Ni (all values are in kG).

Host	Fe	Co	Ni
H_Σ^{Sn}	−870	−611	−198
H_v^{Sn}	+782	+604	+214
H_{calc}^{Sn}	−88	−7	+16
H_{meas}^{Sn}	−88	−26	+16
H_Σ^{Tl}	−1885	−1324	−429
H_v^{Tl}	+1693	+1308	+462
H_{calc}^{Tl}	−192	−16	+33
H_{meas}^{Tl}	−192(70)	−96(85)	...

V. VARIATION OF HYPERFINE FIELD AT Sn AND Tl IN Fe, Co, AND Ni HOSTS

There is a well-known case of change in sign of the hyperfine field at an Sn solute atom which this model explains very well.

We see from Table II that for Sn in Fe the hyperfine-field contributions from H_Σ and H_v are large and of opposite sign. Thus we have a case where the total hyperfine field has the possibility of changing sign with host. In Table V we list the individual contributions to the hyperfine field at an Sn atom as obtained by scaling the values of H_Σ and H_v in the Fe host to Co and Ni hosts by Eqs. (8) and (7a). We see that the calculated values for the total field $(H_\Sigma + H_v)$ agree satisfactorily with the measured values and the change in sign of the hyperfine field at Sn is due to the opposition between the comparable values of H_Σ^{Sn} and H_v^{Sn}.

Since in Sec. II C we mentioned that for Co and Ni the host atoms near a solute atom would be expected to have moment perturbations we must further justify using the scaling, Eqs. (8) and (7a), to obtain H_Σ and H_v in Co and Ni. The majority bands are believed to be full for Ni and nearly full for Co. Thus upon alloying these hosts with nontransition elements, mainly the minority bands receive the added valence electrons. On an atomic scale this would be manifested by the moment on the Co or Ni atoms surrounding the solute atom having their moments decreased, as has been seen in neutron experiments.[42] Such a decrease would decrease the H_Σ and H_v values proportionally. However, these moment decreases are small and since both H_Σ and H_v are proportional to the moments, to first order, their sums would be the same, so we show $H_{calc}^{Sn} = H_\Sigma + H_v$ in the third row of Table V. A correction to the Sn values in Co and Ni by a factor of $1 - \Delta\mu$, where $\Delta\mu$ is some average of the moment changes in the first few neighbor shells, would change the magnitude a little but not the signs of the resultant calculated fields.

Another solute atom where this might happen is Tl. The calculated values for Tl, again scaled from an Fe host, are also listed in Table V. Unfortunately the field at Tl in Ni has not been measured, but we expect it to have changed sign from that in Fe and Co and to be small and around +33 kG.

VI. CONCLUSIONS

We have presented a model for the origin of ferromagnetism in Fe, Co, and Ni which attributes the ferromagnetic coupling to the indirect coupling of the predominately localized moments through a small fraction (~5%) of itinerant d-like electrons. Since neither a direct interaction nor an indirect

interaction through the $4s$ electrons is capable of producing a strong enough coupling to cause the ferromagnetism of Fe, the most plausible mechanism left is an indirect coupling through itinerant d electrons. It is reasoned that for this coupling to be ferromagnetic the k_F values of itinerant d electrons responsible for the coupling must be small, indicating a small number of itinerant d's. We show that hyperfine-field data, Fermi-surface measurements, and band calculations support this model. Moreover, upon reviewing many types of experiments which have been interpreted to indicate itinerant d electrons, we find that they are all consistent with the small degree of itinerancy proposed here, and furthermore many of them even indicate only a small degree of itinerancy.

We also give a model for the origin of the hyperfine field in these metals and their alloys and give scaling rules for each of the three contributions. This model is applied to evaluate various parameters which occur in the different contributions of the hyperfine field and to show that the change in sign of the hyperfine field at Sn in Fe, Co, and Ni matrices is due to the competition between the two large comparable terms of CEP and volume overlap which comprise the hyperfine field at Sn.

The approach that arises from considering hyperfine-field data is that moment perturbations are the more fundamental in determining CEP oscillations. The large spatial extent which sometimes occurs in host-moment perturbations (each moment is mainly localized but the individual moment perturbations fall off with distance from the solute atom) upon alloying arises naturally from the spatial extent of the itinerant d-like CEP. Generally this spatial extent is expected to be larger (for a small number of itinerant d's) than the usual spatial extent of charge-screening oscillations. The charge perturbations are considered to be unimportant or secondary in producing moment perturbations. However, other effects, e.g., the volume-overlap terms, are due primarily to charge perturbations in the sense that they arise because of charge screening. The small spatial extent of the charge perturbation confines the H_v term to depend mainly on near neighbors. Moment perturbations will be discussed extensively in a forthcoming paper.

---

†Various portions of this paper have been presented at the Conference on Hyperfine Interactions in L'Aquila, Italy, 1972 and Conference on Magnetism and Magnetic Materials, Denver, Colo., 1972.

[1]For an extensive bibliography see (a) C. Herring, in *Magnetism*, edited by G. T. Rado and H. Suhl (Academic, New York, 1966), Vol. IV; (b) N. F. Mott, Adv. Phys. **13**, 325 (1964).

[2](a) R. N. Stuart and W. Marshall, Phys. Rev. 120, 353 (1960); (b) A. J. Freeman and R. E. Watson, Phys. Rev. **124**, 1439 (1961); (c)W. J. Carr, Jr., J. Phys. Soc. Jap. Suppl. **17**, 36 (1963); and (d) R. L. Garifullina, M. V. Eremin, and A. M. Leushin, Sov. Phys. Solid State 14, 317 (1972).

[3]C. Zener, Phys. Rev. **81**, 440 (1951); Phys. Rev. **91**, 303 (1953).

[4]M. A. Ruderman and C. Kittel, Phys. Rev. **96**, 99 (1954); T. Kasuya, Prog. Theor. Phys. **16**, 45 (1956); K. Yosida, Phys. Rev. **106**, 893 (1957) (called RKKY).

[5]P. W. Anderson and A. M. Clogston, Bull. Am. Phys. Soc. **2**, 124 (1961); P. W. Anderson, Phys. Rev. **124**, 41 (1961).

[6](a) M. B. Stearns, Phys. Rev. **129**, 1136 (1963); (b) Phys. Rev. **147**, 439 (1966); Phys. Rev. **168**, 588 (1968); (c) M. B. Stearns and S. S. Wilson, Phys. Rev. Lett. **13**, 313 (1964).

[7](a) M. B. Stearns, Phys. Rev. B **4**, 4069 (1971); (b) Phys. Rev. B **4**, 4081 (1971).

[8]M. B. Stearns, Phys. Rev. B **6**, 3326 (1972).

[9]S. Wakoh and J. Yamashita,J. Phys. Soc. Jap. **21**, 1712 (1966).

[10]K. J. Duff and T. P. Das, Phys. Rev. B **3**, 192 (1971); Phys. Rev. B **3**, 2294 (1971), referred to as DD.

[11]A. V. Gold, L. Hodges, P. T. Panousis, and D. R. Stone, Int. J. Magn. **2**, 357 (1971).

[12]J. Friedel, G. Leman, and S. Olszewski, J. Appl. Phys. **32**, 325S (1961).

[13]J. A. Hofman, H. Paskin, K. J. Taner, and R. J. Weiss, J. Phys. Chem. Solids **1**, 45 (1956).

[14]R. D. Lowde, Proc. R. Soc. Lond. **235**, 305 (1956); M. Ericson and B. Jacrot, J. Phys. Chem. Solids **13**, 325 (1960).

[15]C. G. Shull and Y. Yamada, J. Phys. Soc. Jap. Suppl. **17**, 1 (1965); C. G. Shull, in *Electronic Structure and Alloy Chemistry of the Transition Elements*, edited by P. A. Beck (Interscience, New York, 1963), p. 69; R. M. Moon, Phys. Rev. **136**, A195 (1964); H. A. Mook, Phys. Rev. **148**, 495 (1966); R. M. Moon, Int. J. Magn. **1**, 219 (1971).

[16]P. Rhodes and E. P. Wohlfarth, Proc. R. Soc. A **273**, 247 (1963).

[17]Recent measurements [M. L. G. Foy, N. Herman, W. J. Kossler, and C. E. Stronach, Phys. Rev. Lett. 30, 1064 (1973)] of the hyperfine field at μ^+ mesons in Fe allow an extension of the CEP curve [M. B. Stearns (unpublished)] to distances closer than the nearest-neighbor distance. The negative oscillation around 0.7 of the lattice constant is found to be more negative than previously anticipated and yields a net polarization which is smaller than the previous value (Ref. 7).

[18]T. A. Kaplan, Phys. Rev. Lett. **14**, 499 (1965).

[19]R. E. Watson and A. J. Freeman, Phys. Rev. **178**, 729 (1969).

[20]J. Langlinais and J. Callaway, Phys. Rev. B **5**, 124 (1962). Their bibliography lists many other band-structure calculations of Ni.

[21]P. A. Beck and H. Claus, *Conference on Electronic Density of States*, Natl. Bur. Std. Publ. No. 323 (U. S. GPO, Washington, D. C., 1971), p. 557.

[22]E. Fawcett, Adv. Phys. **13**, 139 (1964); W. A. Reed and E. Fawcett, *Proceedings of the International Conference on Magnetism, Nottingham* (The Institute of Physics and Physical Society, London, 1965), p. 120.

[23]C. G. Shull and M. K. Wilkinson, Rev. Mod. Phys. **25**, 100 (1953); J. S. Kasper and B. W. Roberts, Phys. Rev. **101**, 537 (1956); N. Kunitomi, T. Yamada, Y. Nakai, and Y. Fuji, J. Appl. Phys. **40**, 1265 (1969).

[24]A. W. Overhauser, Phys. Rev. **128**, 1437 (1962).

[25]An explanation similar to this was first given by E. C. Stoner

[Rep. Prog. Phys. **11**, 49 (1947).] However, this type explanation was rejected in Ref. 1(b), p. 362 for a much more complex interpretation; it now seems this simpler view is more likely.

[26]See, e.g., J. Crangle, in *Electronic Structure and Alloy Chemistry of the Transition Elements*, edited by P. A. Beck (Interscience, New York, 1963), p. 51.

[27]N. F. Mott, Proc. Phys. Soc. Lond. **47**, 571 (1935).

[28]G. K. Wertheim, V. Jaccarino, J. H. Wernick, and D. N. E. Buchanan, Phys. Rev. Lett. **12**, 24 (1964).

[29]G. Busch, M. Campagna, and H. C. Siegman, Phys. Rev. B **4**, 746 (1971). P. M. Tedrow and R. Meservey, Phys. Rev. B **7**, 318 (1973); W. Gliech, G. Regenfus, and R. Sizmann, Phys. Rev. Lett. **27**, 1066 (1971); C. Rau and R. Sizmann, Phys. Lett. A **43**, 317 (1973).

[30]H. A. Mook and R. M. Nicklow, Phys. Rev. B **7**, 336 (1973); H. A. Mook, R. M. Nicklow, E. D. Thompson, and M. K. Wilkinson, J. Appl. Phys. **40**, 1450 (1969); H. A. Mook, J. W. Lynn, and R. M. Nicklow, Phys. Rev. Lett. **30**, 556 (1973).

[31]See, e.g., J. F. Cooke and H. L. Davis, AIP Conf. Proc. **10**, 1218 (1973).

[32]For an accumulation of data to 1967 see D. A. Shirley, S. S. Rosenbaum, and E. Matthais, Phys. Rev. **170**, 363 (1968); also E. Matthais and D. A. Shirley, *Hyperfine Structure and Nuclear Radiations* (Wiley, New York, 1968). An up-to-date tabulation is given in Table II.

[33]M. Rubinstein, G. H. Stauss, and M. B. Stearns, J. Appl. Phys. **37**, 1334 (1966).

[34]J. J. Murphy, J. I. Budnick, and S. Skalski, J. Appl. Phys. **39**, 1239 (1968); R. H. Dean, R. J. Furley, and R. G. Scurlock, J. Phys. F **1**, 78 (1971); E. F. Mendis and L. W. Anderson, Phys. Status Solidi **41**, 375 (1971); G. Gruner, I. Vincze, and L. Cser, Solid State Commun. **10**, 347 (1972).

[35]P. W. Anderson, Phys. Rev. **124**, 41 (1961); S. Koide and M. Peter, Rev. Mod. Phys. **36**, 160 (1964); R. E. Watson, S. Koide, M. Peter, and A. J. Freeman, Phys. Rev. **139**, A167 (1965).

[36]E. Daniel and J. Friedel, J. Chem. Solids 24, 1601 (1963).

[37]D. J. Kim and B. B. Schwartz, Phys. Rev. Lett. **28**, 310 (1972).

[38]O. Gunnarson, B. I. Lundquist, and S. Lundquist, Solid State Commun. **11**, 149 (1972).

[39]M. B. Stearns, Phys. Lett. A **34**, 146 (1971). It has been brought to my attention that A. V. Kogan {Fiz. Tverd. Tela **9**, 336 (1967) [Sov. Phys.-Solid State **9**, 251 (1967)]} pointed out the dependence of H_z on the ionic radius. However, he did not work out, in detail, the behavior of the H_v term.

[40]As given in *Metals Handbook* (Amer. Soc. for Metals, Cleveland, Ohio, 1948), p. 29. The conversion factor from V to atomic radius is $r_a = 0.736V^{1/3}$.

[41]A. W. Overhauser, J. Appl. Phys. **34**, 1019 (1963); A. W. Overhauser and M. B. Stearns, Phys. Rev. Lett. **13**, 316 (1964).

[42]M. F. Collins and G. G. Low, Proc. R. Soc. Lond. **86**, 539 (1965); J. B. Comly, T. M. Holden, and G. G. Low, Proc. Phys. Soc. Lond. C **1**, 458 (1968).